SIMULATION HELPED POSITIONING OF DEFECTS DETECTED IN CLADDED COMPONENT

G. Haïat[+], P. Calmon[+], and F. Lasserre[#]
+Commissariat à l'Energie Atomique, DRT/LIST, CEA Saclay, FRANCE
Framatome ANP/Intercontrôle, Rungis, FRANCE
guillaume.haiat@cea.fr

Abstract

In industrial applications and especially in nuclear industry, accurate positioning and sizing of defects are a strong requirement for ultrasonic non destructive testing (NDT). Ultrasonic NDT methods are commonly based on the analysis of echoes arising after the propagation and the interaction with scatterers (defects) of an ultrasonic beam radiated in the inspected component. When the surface of the component is not regular, it is well-known that the ultrasonic beam may be seriously perturbed. In some cases the application of simple methods of positioning can consequently give rise to noticeable discrepancies and only the utilization of modeling tools taking into account the component geometry allows to obtain accurate and reliable locations and sizes.

In this paper we present a work made in the context of the ultrasonic inspection of the pressure vessel of French nuclear reactors. The vessel being cladded, the inspected surface may present irregularities. Consequently, a method allowing to accurately locate defects through the cladding has been developed. The method is based on the modeling software developed by CEA in order to predict the propagation and scattering of ultrasounds in the material and the real surface of the vessel is deduced from ultrasonic (L0) measurements and then inputted in the calculations.

Introduction

The ultrasonic inspection of the vessel of French pressurized water reactors (PWR) uses focused transducers acting in pulse echo mode. The inspection aims at detecting and characterizing crack type defects. The vessel being made of ferritic steel, an austenitic cladding is performed on its internal surface to provide corrosion protection. The researched cracks are located below and within this cladding and tip diffraction is the mechanism responsible of the detected echoes. Positioning and sizing of defects are achieved by analysing the location and time of flight of the echoes. In some plants the surface is not grinded and shows irregularities such as grooves due to pass overlaps. These irregularities may generate strong echoes which have been the subject of previous works [1] and are out of the scope of this paper. Moreover, they may significantly perturb the ultrasonic beam transmitted through the cladding and consequently make more difficult accurate positioning and sizing of defects. In addition, the elastic properties of the cladding (austenitic, anisotropic) and the vessel (ferritic, isotropic) are different which affect the location and time of flight of echoes.

The propagation of ultrasonic beams in anisotropic and heterogeneous components [2] and the transmission through an irregular interface [3] can currently be predicted by the models developed by CEA and implemented in the CIVA software [4]. The work presented in this communication aimed at proposing a simulation-helped positioning method based on these tools.

The inspections are performed by using a set of five transducers. Four of them, conceived in order to generate a focused longitudinal beam refracted at 63°, are positioned in two orthogonal planes and two opposite directions in order to detect cracks growing in two perpendicular planes. In addition, one L0° transducer permits to ensure a correct position of the set of transducers relatively to the component surface. The results issued from the L0 transducer are used here to determine the current surface geometry encountered by the wave.

In this communication, we firstly illustrate and explain on one example the effects of the cladding on the echo-structure. We then describe the simulation-helped positioning method which has been developed. Lastly we present results of experiments performed in order to evaluate the method reliability.

Effects of the cladding effects on the echo structure

In figure 1, are presented two experimental Bscan obtained respectively on a planar part and a machined part whose surface is representative of the surfaces encountered on site. The two parts contain a side drilled hole at the same depth. This comparison illustrates the main effects of the irregular surface of the cladding which can be observed on echoes issued from cracks: attenuation, displacement and splitting.

Firstly, looking at the figure 1 it appears that besides the principal echo arising from the defect and involving a pure longitudinal/longitudinal path within steel, supplementary echoes are detected: surface echoes and echoes involving shear waves propagation. The latter are also generated on the planar part but, on the irregular part, they are less attenuated than the pure longitudinal echo. In site, the attenuation of the shear waves within the austenitic cladding strongly reduces the importance of these echoes. More interesting is the analysis of the pure longitudinal echo itself.

The echo attenuation (of 6dB on the presented example) has only influence on the defect detection and not on its positioning and is therefore out of the scope of this paper. On the contrary the displacement of the echo in the Bscan may induce a loss of accuracy when positioning the crack-tip responsible of the echo if the surface irregularity is not taken into account. Moreover, the splitting makes the analysis more difficult and the two echoes could be interpreted as issued from two different scatterers which both would be wrongly positioned.

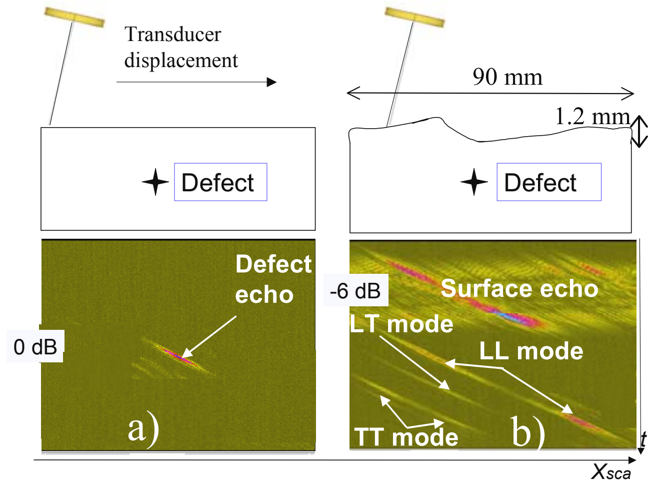

Figure 1 : Real acquisitions of echoes generated by a defect in the component. a): the interface is flat, b): it is complex. Profiles are shown on top of each B-scan, with a different horizontal and vertical scale.

The computation of the ultrasonic fields transmitted within the parts can help to better understand these effects. On figure 2 are shown the field transmitted through the planar part (figure 2a) and through the machined one (figure 2b-g) for different probe positions. In the latter case, the scanning position is indicated by arrows which points on the location of the intersection between the surface profile and the focal axis. The displays are cartographies of the amplitude of the velocity potential. For each cartography is indicated the value in dB of the amplitude maximum relatively to the planar case.

The black star indicates the real position of the defect inside the component. The comparison between the cartography 2a obtained on the planar part and cartographies 2b to 2h shows that the transmitted beam is strongly affected by the surface geometry. Its shape varies from one position to another, depending on the probe position and the surface actually encountered by the wave. For example on figures 2b to 2d we can notice that the transmitted beam is splitted within two main lobes separated by a zone of weak amplitude. This pattern is explained by considering the surface geometry: The central part of the beam encounters an unfavourable slope upon which the incident angle is beyond the critical angle. On both sides of this slope, well oriented parts of the surface allow the forming of the two lobes whose orientation depends on the local normal on the surface.

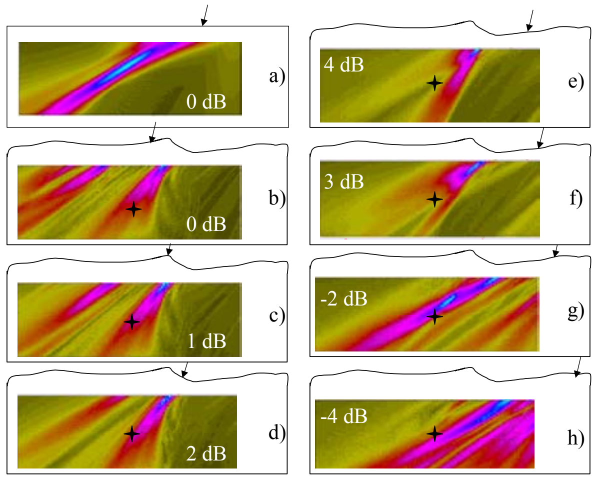

Figure 2 : Effect of surface irregularities on the transmitted beam. Simulated cartographies obtained through a): the planar surface, and b), c), d), e), f), g), h) the irregular surface for different probe positions.

The splitting of the LL echo and the location of its maxima are explained when considering the amplitude incident on the defect versus the probe position. We can see that this amplitude is consequent around positions 2c and around position 2g whereas it drastically decreases between these two positions. These observations are quite coherent with the experimental Bscan since the two maxima of the echo are detected at positions corresponding to figure 2c and 2g.

The austenitic cladding exhibits an orthorhombic symmetry whose characteristics can be found in [5]. Besides the effects of the irregular surface, the effects of the differences between the elastic properties of austenitic and ferritic steels have also been evaluated by computation. Unsurprisingly, it has been observed that not to take into account these differences in the positioning process would induce discrepancies of several millimeters in depth.

The positioning method

Determination of the actual profile and creation of a CAD file

In the aim of accurately positioning an ultrasonic indication, it is required to know the actual surface profile which has been encountered by the wave. The CAD description of this profile is an input of the positioning method and is deduced from the surface echo detected by the L0° transducer. An processing algorithm is applied to the Bscan which uses time of flight measurements to evaluate a set of altitude values. From this set of samples, a faceted surface is created after application of a smoothing algorithm in the aim of minimizing the number of facets. The extraction procedure has been tested on several samples whose profiles were known. Figure 3 illustrates an example of such validation on a representative sample and shows the good agreement between the real and extracted profiles.

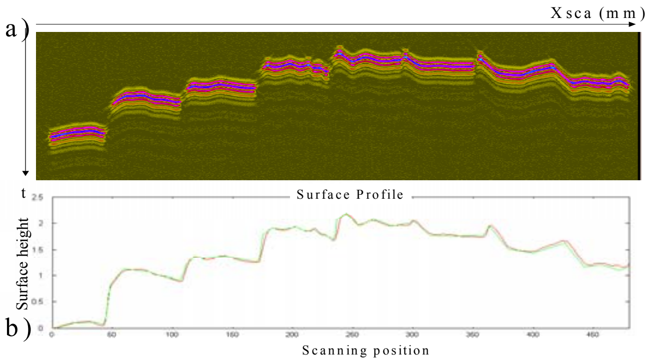

Figure 3. a): L0° B-scan. b): Comparison between the real (in dark) and extracted (in light) profiles.

From this profile and the knowledge of the cladding characteristics (depth and elastic constants) a 3D CAD file describing the inspected component is created by extrusion or revolution depending on the inspected part of the vessel.

Processing of the experimental Bscan:
The successive stages of the positioning method are schematized on figure 4. The starting point of the method is the choice, on an experimental B-scan of the echo that will be processed and the extraction of its position (X,T) in the scanning/time of flight space. These two parameters will be the main inputs of the method. In order to make reproducible from one operator to another, the determination of X and T is performed automatically. The *CIVA* segmentation algorithm is applied on the Bscan with a pre-determined set of parameters. The segmented Bscan is constituted of a set of echoes, described as segments (see Figure 4b). A segment is a set of linked points located respectively at (X_i, T_i), each of them being associated to an amplitude value. From one given echo, the couple (X, T) are the coordinates of the point belonging to the segment whose amplitude is maximum.

Field computation and determination of a set of possible loci
In order to determine the possible loci of the scatterer responsible of the echo detected at (X,T), a 3D *CIVA* field computation is carried out. From the X value, the L63° transducer is positioned relatively to the CAD description. The applied model, based on geometrical elastodynamic approximation and pencil method has been described in several communications (see for example [2]). An example of computation result is shown on figure 4c. The computed quantity is the auto-convolution of the velocity potential, from which is extracted a "time of flight" at every point of the zone. The researched loci are then obtained by carrying out a comparison of these times of flight with time T and an application of an amplitude threshold. The output of this post-processing (see figure 4d) is a set of N sampled couple of values (x, z), (x, z) being the coordinates in the plane of incidence. The z-axis is the depth axis, perpendicular to the x-axis. Typically, N is in the 10-50 range for a required accuracy of 0.2 to 0,1 mm.

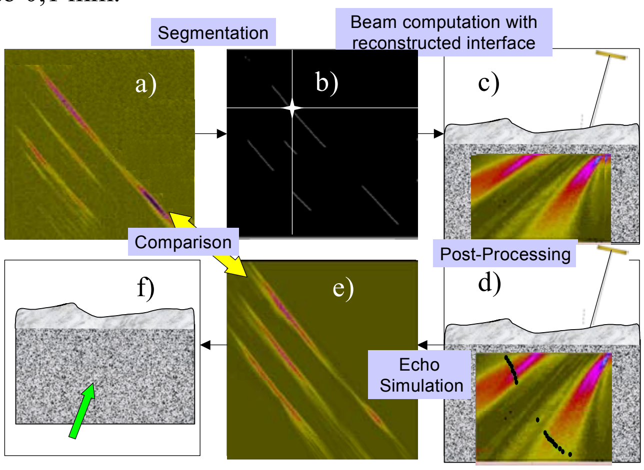

Figure 4 : Schematic presentation of the positioning method a): The experimental B-scan. b): The segmented echo and its (X,T) coordinates. c): Field calculation at X. d): The set of possible loci e): One simulated B-scan. f): Choice of the best locus.

Determination of the final scatterer position
The final scatterer position, output of the method, is obtained by selecting the "best" locus in this set (figure 4e and f). This is done by comparing the experimental and the N simulated segmented Bscans corresponding to the N loci of the set. This is done by using the simulation ultrasonic module of *CIVA*. To model crack tips response, the scatterer, is here assumed to be a linear scatterer located at (x,z) and large relatively to the incident beam. This simple model which neglects the directivity of the field scattered by a crack tip allows faster computations. The approximation is quite sufficient since the comparisons between the simulated and the experimental Bscan relies on comparison between the position of the different maxima observed on the segments and not on their absolute amplitudes.

Experimental validation
In order to validate the method, an experimental campaign has been launched. We present here the results obtained on two sets of experiences. The first one has been carried out on a non cladded part whose machined surface is representative of the internal

vessel surface. Five ∅ 2 mm side drilled holes have been implemented in the part. The locations of these holes have been chosen in order to favor worst cases: they correspond to the strongest perturbations of the ultrasonic field. In table 1 have been reported the positions obtained by carrying out the method described above and the real positions of the holes.

Table 1 : Comparison between obtained and real positions of the five drilled holes. *Δx* and *Δz* are respectively the discrepancies observed on lateral location and depth.

Defect #	Obtained Position (mm)	Real Position(mm)	ΔX (mm)	ΔZ (mm)
1	111.6;31.6	111.7;30.6	-0.1	1.
2	160.1;30.45	160.7;30.45	-0.6	0.
3	229.1;18.8	230.7;20.6	-1.6	-1.8
4	296.5;21.6	296.7;20.8	-0.2	0.8
5	332.3;21.35	332.8;20.75	-0.5	0.6

The good agreement both on lateral location x and depth z can be noticed. We can see that, excepted in the case of the defect 3, the Δx or Δz discrepancies are lower or equal to 1 mm. In the case of defect 3 the higher values of the discrepancies appear to be due to interferences with a strong surface echo.

A second set of experiments have been performed on a planar cladded part, in order to evaluate the ability of the method to take into account anisotropy effects in the cladding. Both cladding and bulk material are identical to the vessel materials. In order to simulate crack tips responses at various depths, several breaking notches of different heights from 10 to 30 mm have been machined. Again, the predicted and real positions show a good agreement, the mean value of discrepancy being 0.5 mm.

Conclusion

In this communication we have presented a method developed in the aim of accurately locating and sizing cracks within the vessel of PWR nuclear reactors. These cracks are detected by tip diffraction mechanism through an austenitic cladding whose surface is possibly irregular. The method applies the ultrasonic models implemented within the *CIVA* software First experiments on calibrated parts show the capability of the method to account for both anisotropy and surface effects. Qualification of the method by application on real on-site acquisitions are now in progress.

References

[1] N. Gengembre and A. Lhémery. “Calculation of wideband ultrasonic field radiated by water coupled transducers into anisotropic media.” in Review of progress in quantitative NDE, ed by D.O. Thomson and D.E. Chimenti, 1998, Vol 17 (Plenum, N-Y), pp. 899-906.

[2] N. Gengembre and A. Lhémery. “Calculation of wideband ultrasonic field radiated by water coupled transducers into heterogeneous media.” in Review of progress in quantitative NDE, ed by D.O. Thomson and D.E. Chimenti, 1999, Vol 18 (Plenum, N-Y), pp. 1131-1138.

[3] N. Gengembre and A. Lhémery. “Calculation of wideband ultrasonic field radiated by water coupled transducers into heterogeneous and anisotropic media.” In Review of progress in quantitative NDE, ed by D.O. Thomson and D.E. Chimenti, 1998, Vol 17 (Plenum, N-Y), pp. 899-906.

[4] S. Chatillon, A. Lhémery, F. Cartier and P. Calmon “CAD-based simulation and imaging tools for UT expertise.” in Review of progress in quantitative NDE, ed by D.O. Thomson and D.E. Chimenti, 2000, Vol 20 (Plenum, N-Y), pp. 710-717.

[5] R.J. Hudgell. “ Handbook on the ultrasonic examination of austenitic clad steel component”, 1994, publislished by European Commission, Joint Research Centre, Institute of advanced materials.